DOI: 10.1002/asia.200600229

Self-Assembled Aggregates and Molecular Bilayer Films of a Double-Chain Fullerene Lipid: Structure and Electrochemistry

Hiroto Murakami,[b] Takashi Nakanishi,[c] Makoto Morita,[b] Naoya Taniguchi,[b] and Naotoshi Nakashima*[a]

Abstract: The self-aggregation behavior of C_{60} fullerenes that bear two octadecyl chains (lipid **1**) as well as the structures and electrochemical properties of cast films of **1** are described. We also examined the self-aggregation behavior in organic solvents of three previously reported compounds: C_{60} with three each of hexadecyl (lipid **2**), tetradecyl (lipid **3**), or dodecyl (lipid **4**) chains. The fullerene lipids in alcohols spontaneously formed spherical aggregates, whose diameters are related to the alkyl-chain lengths, concentrations of the fullerene lipids, and the solvent polarity. The morphologies of the aggregates showed temperature dependence. Cast films of **1** formed multimolecular bilayer structures that undergo a phase transition typical of lipid bilayer membranes. The electrochemistry of cast films of **1** on an electrode in aqueous medium exhibits temperature dependence.

Keywords: aggregation · electrochemistry · fullerenes · lipids · supramolecular chemistry

Introduction

Much attention has been focused on the chemistry and physics of fullerenes and their derivatives,[1–5] while the construction of hybrid materials of fullerenes and functional compounds is also of interest.[6–11] We and others have been interested in combining fullerene chemistry and the chemistry of lipid bilayer membranes.[12–24] Study of this subject is expected to open up an exciting area of science. We already reported that water-insoluble C_{60}-bearing lipids (fullerene lipids **2**–**4**) with triple C_{16}, C_{14}, or C_{12} alkyl chains form organized multibilayer films; these films undergo phase transitions attributable to a lipid bilayer phase transition that is more typically observed in liposomal and synthetic lipid bilayer membranes and/or to a change in orientation of the C_{60} moieties.[21] We also demonstrated the unique electrochemical properties of cast films of fullerene lipids[21,22] and of C_{60}/artificial ammonium-lipid composites[12–19] on electrode surfaces.

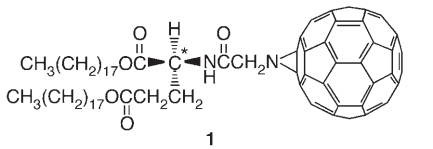

1

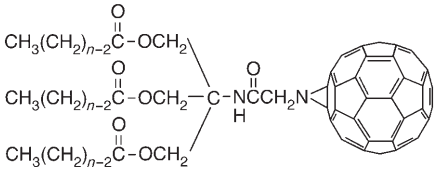

2: n=16
3: n=14
4: n=12

Self-assembled superstructures of lipids have also attracted a great deal of attention in the field of nanoscience. In particular, superstructures of fullerenes are of interest be-

[a] Prof. N. Nakashima
Department of Applied Chemistry
Graduate School of Engineering
Kyushu University
744 Motooka, Fukuoka 819-0395 (Japan)
Fax: (+81) 92-802-2840
E-mail: nakashima-tcm@mbox.nc.kyushu-u.ac.jp

[b] Dr. H. Murakami, M. Morita, N. Taniguchi
Department of Science and Technology
Graduate School of Materials Science
Nagasaki University
Nagasaki 852-8521 (Japan)

[c] Dr. T. Nakanishi
Supermolecules Group, Organic Nanomaterials Center (ONC) and International Center for Young Scientists (ICYS)
National Institute for Materials Science (NIMS)
Tsukuba 305-0044 (Japan)

Supporting information for this article is available on the WWW under http://www.chemasianj.org or from the author.

cause of their unique chemical and physical properties.[10,12,25] A variety of strategies for the formation of fullerene superstructures have been proposed and developed by many researchers.[20,26–43] For instance, we described the formation of fibrous and disklike superstructures from a C_{60}-bearing ammonium amphiphile with a long alkyl-chain spacer.[20]

Morphological variation of self-assembled fullerene superstructures through external stimuli such as solvent polarity,[42,44–47] pH,[33,39] temperature,[32] and light has also been the subject of intense research in recent years because of the possibility for exploitation of the advantageous intrinsic properties of fullerenes, for example, photochemical and photophysical properties and electrochemistry. Tam and co-workers reported that the aggregates of C_{60}-containing poly(2-(methylamino)ethyl methacrylate) change their morphologies according to pH and temperature.[32] Patnaik and co-workers reported a fullerene derivative with long alkyl chains that forms self-aggregates in binary mixtures of solvents whose dielectric constants exceed a critical value of around 30.[48] More recently, Nakanishi et al. reported that a fullerene derivative with long alkyl chains forms hierarchically ordered superstructure assemblies with well-defined 1D, 2D, and 3D architectures such as vesicles, fibers, disks, and cones.[49]

Herein, we designed and synthesized an L-glutamate-based chiral fullerene lipid **1** with double octadecyl chains to investigate the effect of the multiplicity of alkyl chains on the lipid and of the existence of a chiral carbon atom on the self-aggregation properties and film structures of the fullerene lipid, as well as the electrochemistry of the lipid films. The cross-sectional area of the double chain in **1** (0.42 nm^2) is smaller than that of the C_{60} moiety (0.78 nm^2),[23,50] whereas the area of the triple-chain moieties in **2**–**4** (0.72 nm^2) is close to that of the C_{60} moiety (see Supporting Information). The number of alkyl chains should influence the fundamental properties of the fullerene lipids. Herein, we describe in detail 1) the self-aggregation properties of **1**–**4** in alcohols, 2) the structure and phase-transition behavior of cast films of **1**, and 3) the temperature-dependent electrochemistry of cast films of **1**.

Results and Discussion

Self-Aggregation Behavior of Fullerene Lipids in Alcohols

A film made from a reddish-brown solution of **1** in chloroform was heated in 2-propanol (or ethanol) at 50 °C for 2 h to obtain a transparent yellowish-brown dispersion. Dispersions of the same color were also obtained from all other fullerene-lipids (**2**–**4**) films.

The UV/Vis absorption spectra of **1** in chloroform and in 2-propanol are shown in Figure 1a. The spectrum of **1** in chloroform shows two strong peaks at 256 and 323 nm together with a very weak peak at 422 nm. The peaks at around 260 and 320 nm arise from the C_{60} moiety in each fullerene lipid and are assigned to the electronic transitions

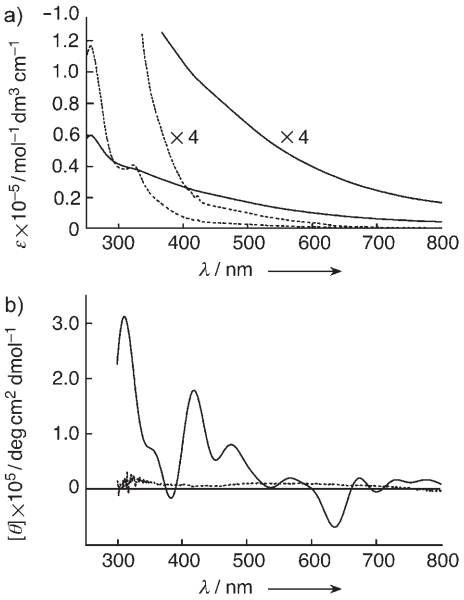

Figure 1. a) UV/Vis absorption and b) CD spectra of **1** in chloroform (----) and 2-propanol (——). [**1**] = 1.6×10^{-5} M for UV/Vis spectra, [**1**] = 1.6×10^{-5} M in 2-propanol and [**1**] = 2.5×10^{-5} M in chloroform for CD spectra.

$1^1A_g\rightarrow6^1T_{1u}$ and $1^1A_g\rightarrow3^1T_{1u}$, respectively.[51] The absorption peak at around 420 nm is characteristic of monosubstituted fullerene derivatives.[52–55] The positions and relative intensities of the peaks in the spectrum of **1** in chloroform are in good agreement with those in *n*-hexane, which suggests that **1** dissolves in chloroform in a nonaggregated form. In contrast, the spectrum of **1** in 2-propanol is very broad, although the peak positions are almost identical to those of **1** in chloroform. Furthermore, the absorbance of the 2-propanol dispersion in the visible region is much larger than that in chloroform, which results in the color change. The same spectral behavior was observed for the other fullerene lipids in both solvents (for **2**, see Supporting Information). The spectral behavior observed is due to the difference in the microscopic environment of the fullerene lipids in these solvents and suggests spontaneous aggregate formation in 2-propanol. In fact, the absorption spectra for aggregates of fullerenes and fullerene derivatives were reported to be broad compared to those of the respective nonaggregated forms.[42,44,47,56]

The CD spectra of **1** in chloroform and in 2-propanol are shown in Figure 1b. Despite the presence of a chiral carbon atom in **1**, a CD band was not detected in a solution of **1** in chloroform, in which **1** does not form an aggregate. In contrast, CD bands for **1** in 2-propanol appear over a wide range of wavelengths, from 300 to 800 nm. These bands could be due to exciton coupling of the highly conjugated π-electron system of the fullerene moiety of **1**-aggregates that possess chirality. The contribution of linear dichroism of **1** aggregates in 2-propanol is almost negligible. Fullerene lipid **2** gave no CD signal even when dispersed in 2-propanol, in which **2** forms spontaneous aggregates, because of the ab-

sence of a chiral carbon atom in **2** (see Supporting Information).

The shape of the fullerene lipid aggregates was characterized with transmission electron microscopy (TEM), scanning electron microscopy (SEM), and atomic force microscopy (AFM). Figure 2 shows typical TEM and SEM images of **1** in 2-propanol. In both images, uniform spherical aggregates can be seen. None of the expected helical aggregates, which would reflect the existence of the chiral carbon atom in **1**, were observed. The thickness of the walls of the spherical aggregates is approximately 10 nm (Figure 2a, inset). A molecular length of 3.8 nm for **1** was estimated from Corey–Pauling–Koltun (CPK) space-filling models, so it is clear that the aggregates have multibilayer morphology. TEM and AFM images of **2** in 2-propanol also showed spherical aggregates (see Supporting Information). Moreover, spherical aggregates were also observed in the TEM images of **3** and **4** in 2-propanol as well as those of **1**–**4** in ethanol. Unlike the double-[57] and triple-chain[58] synthetic amphiphiles and the water-soluble fullerene[20] reported previously, however, fibrous and disklike aggregates were not formed. These results suggest that there is no relationship between the molecular shape of the fullerene lipids and the shapes of their aggregates.

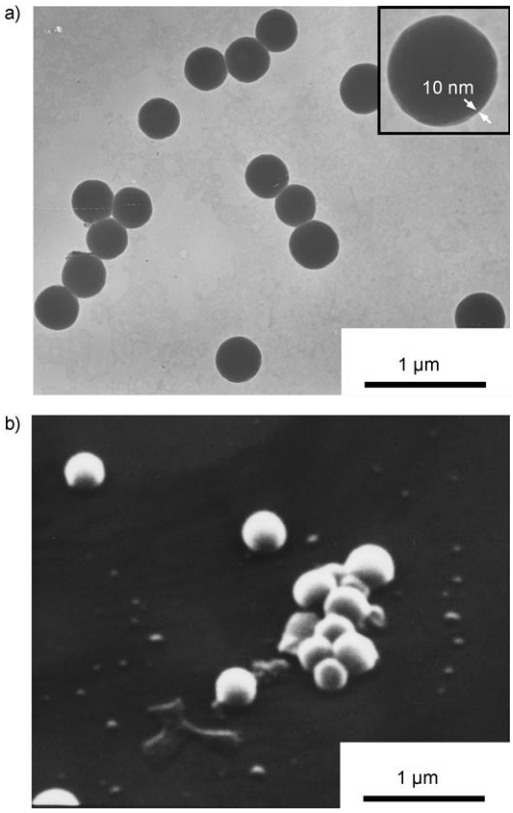

Figure 2. a) TEM and b) SEM images of **1** in 2-propanol.

A dynamic light scattering (DLS) study was conducted to obtain information about the size of the aggregates of the fullerene lipids in the dispersions (for the data, see Supporting Information). The results are summarized in Table 1. For the aggregates of **2** in 2-propanol and in ethanol, the size of the aggregates increases as the concentration of the fullerene lipid in the dispersion increases. For instance, the size of **2** aggregates in a 30-μM dispersion in 2-propanol is 540 nm, which is larger than that in an 18-μM dispersion (200 nm), whereas those of 24-μM and 14-μM dispersions in ethanol are 415 and 320 nm, respectively. At the same time and in contrast to the aggregates of **1**–**4** in 2-propanol, the size of the aggregates increases with an increase in alkyl-chain length of the lipid rather than concentration, that is, the sizes of **1** (16 μM), **2** (18 μM), **3** (22 μM), and **4** (21 μM) are 390, 200, 105, and 95 nm, respectively. Therefore, it was found that the variation of the sizes of the aggregates depends both on the alkyl-chain length and the concentration of the fullerene lipids in the dispersions. These two factors also affect the monodispersity, which increases upon decreasing the alkyl-chain length and increasing the concentration. This effect may come from the conformation of the alkyl-chain moieties of the fullerene lipids; that is, a shorter chain length easily enables the *gauche* conformation, leading to weaker packing through van der Waals interactions. The increase in solvent polarity also results in an increase in aggregate size. Similar phenomena were described for fullerenes with different chemical structures.[42,44–47]

To investigate the thermal stability of the aggregates, we also performed DLS and TEM measurements for the dispersions **3** and **4**. The DLS data are shown in the Supporting Information and are summarized in Table 2. The sizes of the

Table 1. Average particle sizes, size distributions, and monodispersities of fullerene lipid aggregates in alcohols determined by DLS measurements.[a]

Fullerene lipid	Film quantity [nmol][b]	Concentration [μM][c]	Solvent	Average particle size [nm]	Size distribution [nm]	Monodispersity dw/dn[d]
1	200	16	2-propanol	390	250–500	1.07
2	200	18	2-propanol	200	110–340	1.08
	400	30	2-propanol	540	350–800	1.20
	200	14	ethanol	320	200–500	1.10
	400	24	ethanol	415	250–700	1.20
3	400	22	2-propanol	105	50–300	1.18
	400	10	ethanol	160	50–500	1.21
4	400	21	2-propanol	95	50–250	1.22
	400	10	ethanol	140	50–400	1.37

[a] DLS measurements were carried out at (25±0.5)°C. [b] Concentration of each stock solution of the fullerene lipid was 1 mM. [c] Concentrations of the dispersions were determined according to the method in the Experimental Section. [d] n = Number average particle diameter, w = weight average particle diameter.

CHEMISTRY
AN ASIAN JOURNAL

Table 2. Average particle sizes of fullerene lipid aggregates in alcohols before and after thermal treatment determined by DLS measurements.[a]

Fullerene lipid	Solvent	Average particle size [nm] A	B[b]	C[c]	D[d]	E[e]
3	2-propanol	105	115	220	3300	150
	ethanol	160	155	330	5080	230
4	2-propanol	95	92	230	3470	175
	ethanol	140	140	330	4750	225

[a] The DLS measurements were carried out at (25±0.5)°C. [b] After keeping A at 25°C for 5 days. [c] After cooling B at 5°C for 1 day. [d] After cooling C at 5°C for another 5 days. [e] After heating D at 50°C for 5 h.

aggregates of **3** and **4** in 2-propanol and ethanol remained constant after storage at 25°C for more than 5 days (average diameter = 95–160 nm). In contrast, in solutions cooled at 5°C for 1 day, the size of the aggregates increased (average diameter = 220–330 nm), and the average size reached 3300–5100 nm after cooling at 5°C for 6 days. The enlarged aggregates persisted even after warming to 25°C. However, a further increase in temperature decreased the aggregate size; that is, at temperatures over 35°C, the size gradually decreased, and on heating at 50°C for 5 h, it was further lowered to 150–230 nm, which is close to the original size of the aggregates (see Supporting Information). Figure 3 shows typical temperature-dependent TEM images of the aggregates of **3** in 2-propanol. In the TEM image in Figure 3b, fused spherical aggregates are clearly visible. It is evident that the increase in aggregate size for the samples prepared by the cooling process is due to fusion of the aggregates. Warming of the fused aggregates at 50°C for 5 h caused the reappearance of the original spherical aggregates. It is now evident that spherical aggregates of the fullerene lipids fuse by cooling at 5°C and are returned to the pristine spherical state by heating at 50°C. Similar temperature-dependent aggregation behavior was observed for **3** in ethanol and for **4** in 2-propanol and in ethanol. The observed aggregation behavior could be due to the temperature dependence of interactions between fullerene moieties.

Fullerenes are known to polymerize under UV irradiation, during which covalent cyclobutane linkages are formed between the fullerene molecules.[59–61] We examined the effect of photoirradiation on the fullerene-lipid aggregates. A dispersion of **2** in 2-propanol containing the spherical aggregates was irradiated with a high-pressure mercury lamp in the absence of a cut filter for 10 h. The dispersion clearly lost color after the irradiation, and no precipitate was produced. The UV/Vis absorbance of the dispersion of **2** after irradiation decreased, and a blue shift of the absorption edge together with the disappearance of the characteristic peaks assigned to the fullerene moiety in **2** were observed, as was expected from the color change of the dispersion (see Supporting Information). In the Raman spectrum of the dispersion of **2** after irradiation, the vibration peak assigned to the carbon–carbon double bonds of the fullerene moiety of **2** was shifted to lower frequency by 18 cm^{-1}. As shown in Figure 4, we observed fused and defective clusters

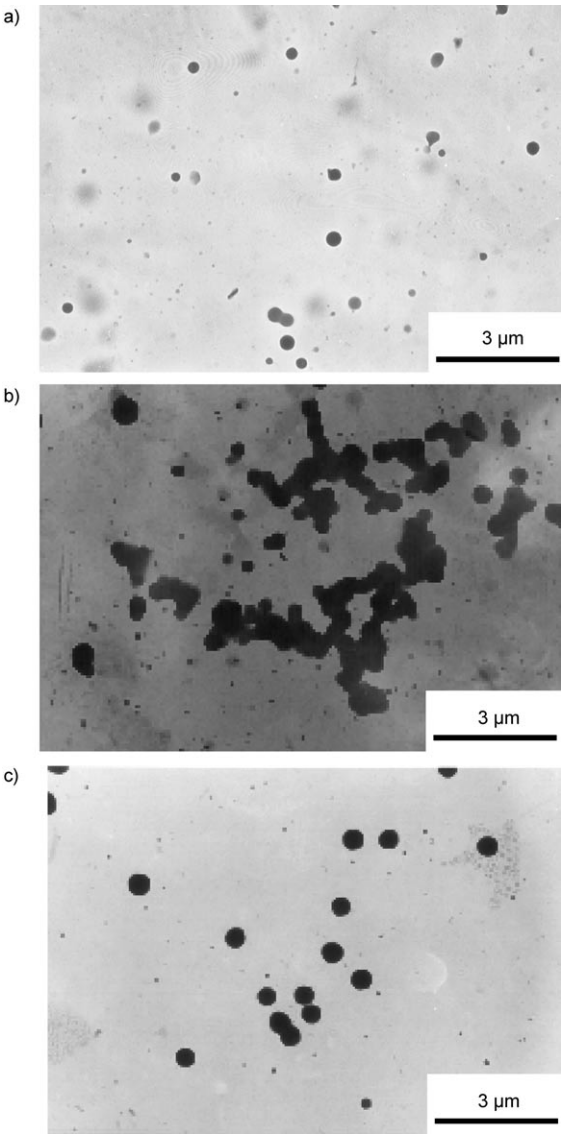

Figure 3. TEM images of **3** in 2-propanol a) before thermal treatment, b) after cooling at 5°C for 5 days, and c) after subsequent heating at 50°C for 5 h.

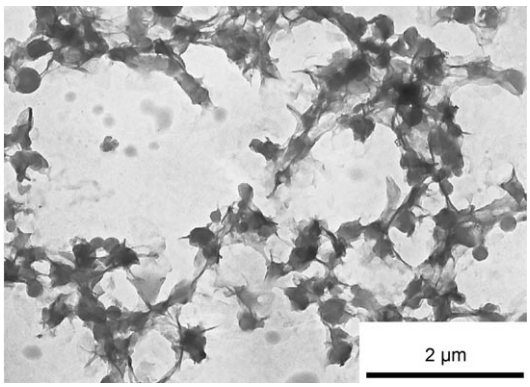

Figure 4. TEM image of **2** in 2-propanol after UV irradiation for 10 h at ambient temperature.

in the TEM images of the **2** aggregate following irradiation; the spherical aggregates were difficult to observe. Thus, UV irradiation causes a partial destruction of the π-electron system of the fullerene moieties, resulting in the formation of fused and defective clusters in the dispersion.

Properties of Fullerene Lipid Films

We have already described the properties of cast films of **2**–**4** examined by differential scanning calorimetry (DSC), UV/Vis and FTIR spectroscopy, and XRD.[21,24] The pertinent features are summarized as follows. 1) Cast films of **2** exhibit two endothermic peaks in the temperature ranges of 35–40 °C (main transition) and 47–49 °C (subtransition) in air, water, and aqueous tetraethylammonium chloride (TEAC; 0.5 M), whereas cast films of both **2** and **3** each showed one endothermic peak at 50–57 °C. 2) Taken together with the results of the temperature-dependent FTIR and UV/Vis spectra of the cast films of **2**–**4**, the main peak in the DSC thermogram of a film of **2** is attributed to the typical phase transition seen in lipid bilayer membranes,[62] and the subendothermic peak of **2** and the peaks of **3** and **4** come from the change in the orientation of the C_{60} moieties. 3) The XRD pattern for each cast film of **2**–**4** shows a diffraction peak corresponding to the (001) plane, suggesting the formation of molecular bilayer membrane structures.

To characterize the cast films of **1**, DSC, FTIR and UV/Vis spectroscopy, and XRD measurements were carried out. The DSC thermogram of a cast film of **1** in air shows a broad endothermic peak at 40.8 °C ($\Delta H = 25.2\ kJ\,mol^{-1}$) (Figure 5a). This DSC behavior, which differs from that for the cast films of **2**, could be due to an increase in the phase-transition temperature for the alkyl-chain moieties caused by increasing the alkyl-chain length, while the subtransition temperature for the change in the orientation of the C_{60} moieties is not affected. The phase transition for the film appears at 39.6 °C ($29.8\ kJ\,mol^{-1}$) in water and at 40.0 °C ($22.4\ kJ\,mol^{-1}$) in aqueous TEAC, thus indicating that the fullerene lipid retains similar molecular orientations in these different media.

In the temperature dependence of the FTIR spectra of cast films of **1** in air, the frequency of the asymmetric and symmetric methylene stretching peaks changes drastically near 40 °C (Figure 5b). The shift of $\tilde{\nu}_{as}(CH_2)$ and $\tilde{\nu}_{s}(CH_2)$ from 2918.8 and 2850.1 to 2922.7 and 2851.8 cm^{-1}, respectively, can be ascribed to the *trans*→*gauche* conformational change of the long alkyl chains,[63,64] which leads to a phase transition in the thin film. The UV/Vis spectrum of the film in air at 25 °C shows three bands with absorption maxima at 219.5 (band A), 265.5 (band B), and 330.5 nm (band C); the peak maxima for bands A, B, and C are shifted to longer wavelengths by 10.5, 10.0, and 8.0 nm, respectively, compared to those in *n*-hexane. These shifts imply the existence of an electronic interaction between the C_{60} moieties in the film. Upon increasing the temperature to 40 °C, the peak maxima for the three bands shifted drastically to shorter wavelengths (Figure 5c). Thus, it is evident that the endothermic peak at 40.8 °C ($=T_c$) in the DSC thermogram of the film of **1** can be attributed to a bilayer phase transition typically observed for liposomal and synthetic lipid bilayer membranes as well as to a change in orientation of the C_{60} moieties. The XRD study revealed that cast films of **1** give a diffraction peak at $2\theta = 1.7°$ (see Supporting Information), which is attributed to the diffraction from the (001) plane with a *d*-spacing value of 5.2 nm. As the molecular length of **1** is about 3.8 nm, the cast films of **1** probably form a biomembrane-mimetic multibilayer structure with the molecular layer tilted by 43° from the normal plane. From these data, we can propose a schematic model for the structure and phase-transition behavior of cast films of **1** (Supporting Information). Below T_c, the lipid forms a rigid crystalline state, in which all alkyl chains have a *trans* conformation. Above T_c, the lipid film reaches a fluid state with a less-ordered structure in which the alkyl chains have a *gauche* conformation and the orientation of the C_{60} moieties is disordered. This mechanism is different from that of the triple-chain fullerene lipid **2** (see Supporting Information).

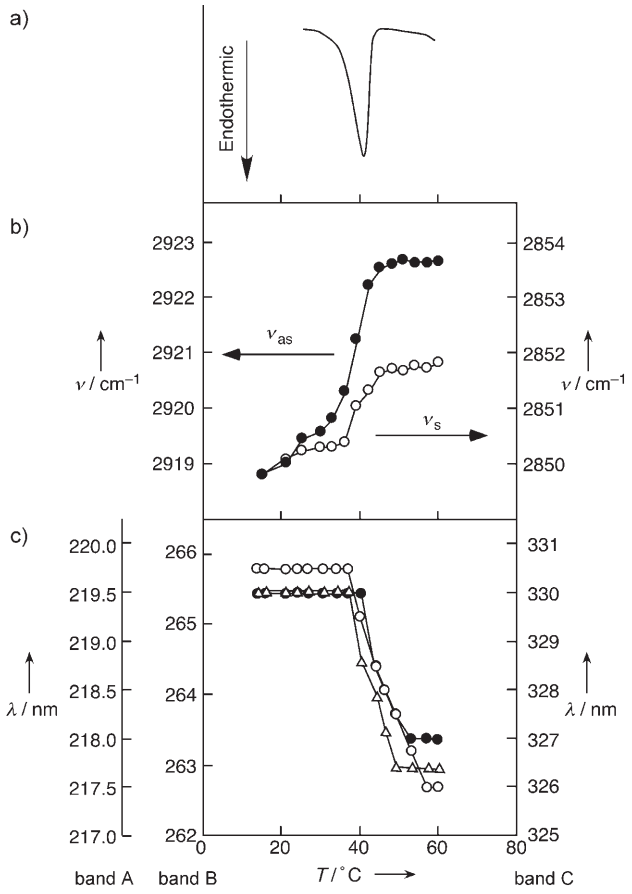

Figure 5. a) DSC thermogram of a cast film of **1** in air. b) Plots of frequency of asymmetric and symmetric CH_2 stretching bands in the FTIR spectra of a cast film of **1** as a function of temperature. c) Plots of wavelengths for band A (●), band B (△), and band C (○) in the UV/Vis spectra of a cast film of **1** as a function of temperature.

CHEMISTRY
AN ASIAN JOURNAL

Electrochemistry

Figure 6a and b show a typical cyclic voltammogram (CV) and differential pulse voltammogram (DPV), respectively,

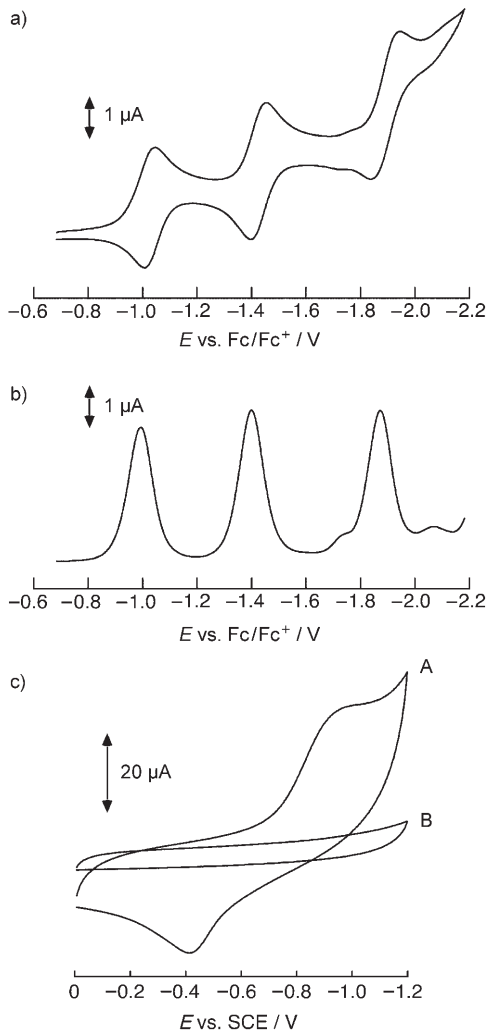

Figure 6. a) CV and b) DPV for **1** (0.5 mM) in dichloromethane containing tetrabutylammonium perchlorate (0.1 M) at 25 °C. Scan rate = 50 mV s^{-1} for CV, scan rate = 5 mV s^{-1}, pulse amplitude = 50 mV for DPV. c) CVs at a scan rate of 100 mV s^{-1} for a cast film of **1** on a BPG electrode in aqueous TEAC (0.5 M) at 45 °C (A) and 15 °C (B).

for a solution of **1** (0.5 mM) in dichloromethane containing tetrabutylammonium perchlorate (0.1 M) as a supporting electrolyte. Three redox couples are evident and correspond to C_{60}/C_{60}^{-}, C_{60}^{-}/C_{60}^{2-}, and C_{60}^{2-}/C_{60}^{3-}. The formal potentials obtained were −1.02, −1.43, and −1.90 V versus ferrocene/ferrocenium (Fc/Fc^+) for $E_1^{0'}$, $E_2^{0'}$, and $E_3^{0'}$, respectively. These potentials are shifted in a negative direction by about 20, 30, and 60 mV for the first, second, and third redox potentials, respectively, compared to those of C_{60} in dichloromethane (−1.00, −1.40, and −1.84 V for $E_1^{0'}$, $E_2^{0'}$, and $E_3^{0'}$, respectively). This shift arises from the closed 6/6 ring bridged structure of the monosubstituted C_{60}, which results in a variation in the number of electrons in the π system of the fullerene moiety from 60π to 58π. The CV and DPV of a solution of **2** in dichloromethane also show three redox couples corresponding to C_{60}/C_{60}^{-}, C_{60}^{-}/C_{60}^{2-}, and C_{60}^{2-}/C_{60}^{3-} at −1.02, −1.43, and −1.94 V, respectively, whose formal potentials are close to those of **1** (see Supporting Information) essentially because of the presence of the same π system.

We previously reported that the electrochemistry of C_{60} embedded in an artificial lipid film[18] or a film of **2**[21] can be tuned with the temperature-controlled phase transition. CV measurements of a cast film of **1** on a basal plane pyrolytic graphite (BPG) electrode were performed at 15 °C (below T_c) and 45 °C (above T_c) and revealed that the electrochemistry of films of **1** on an electrode shows strong temperature dependence. Below T_c, the modified electrode gave no electrochemical response attributable to the C_{60} moiety in **1**, whereas above T_c, a cathodic peak at −0.9 V and an anodic peak at −0.42 V versus a saturated calomel electrode (SCE) were observed (Figure 6c). These peaks are, however, unstable on potential cycling, which suggests the formation of an electrochemically inactive film of **1** at the electrode surface. Because of this instability in the CV measurements, we used Osteryoung square-wave voltammogram (OSWV) measurements to evaluate the effect of the phase transition of the fullerene films on the electrodes. Typical OSWVs for a **1**-modified electrode in water containing TEAC as an electrolyte is shown in the Supporting Information. The Faradaic current at temperatures below 20 °C is very small, although the current increases upon increasing the temperature. Plots of the reduction current as a function of temperature (Figure 7) give a break near 38 °C, which is close to the phase-transition temperature of a film of **1**, which suggests that the phase transition of this film affects the electrochemistry of the modified electrodes, that is, the fluid lipid phase provides a suitable microenvironment for the electrochemistry of the fullerene moieties of films of **1**. The evident direct electrochemical communication of the fullerene moiety with the electrode would be due to the enhanced diffusion rates of the electrolytes and **1** molecules in the fluid phase. On the contrary, the electrochemistry was hindered in the rigid lipid bilayer phase.

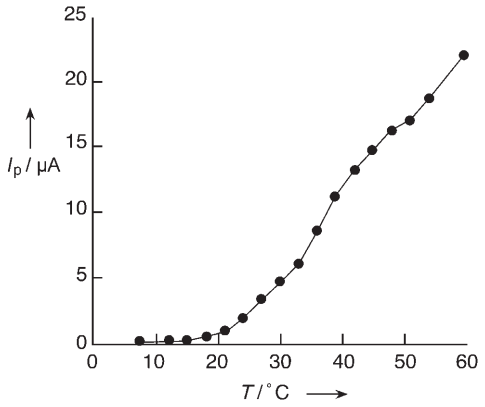

Figure 7. Plot of peak current in the OSWV of a cast film of **1** on a BPG electrode in aqueous TEAC (0.5 M) as a function of temperature.

Conclusions

We have described herein 1) the formation of the fullerene-lipid aggregates **1**–**4** in alcohols together with their properties, including thermal behavior and the effect of photoirradiation on the aggregates in solution, and 2) the structure and electrochemistry of films of the fullerene lipid **1**. Spectroscopic studies indicated that the fullerene lipids **1**–**4** self-assemble spontaneously in 2-propanol and in ethanol. Electron and atomic force microscopic investigations revealed that, regardless of the number of alkyl chains, the fullerene lipids used in this study form spherical aggregates in alcohols. CD activity was observed for the dispersions. From the DLS studies, the size of the aggregates depends on the alkyl-chain length and concentration of the fullerene lipid as well as the solvent polarity. Thermal treatment or photoirradiation of the lipid dispersions causes morphological changes. DSC, FTIR and UV/Vis spectroscopy, and XRD measurements revealed that **1** forms a multibilayer structure with a phase transition coupled to the change in orientation of the C_{60} moieties. The electrochemistry of a film of **1** can be tuned the temperature-controlled phase transition of the film.

The present study could provide useful information towards the understanding of fullerenes in their aggregated/organized states and their potential application in the field of nanoscience and technology.

Experimental Section

Materials

The synthesis of **1** is described in the Supporting Information. Fullerene lipids **2**–**4** were prepared according to our previously reported methods.[20] All solvents used in this study were of spectroscopic grade. Other chemicals used were of reagent grade.

Preparation of Fullerene-Lipid Dispersions in Alcohols

A solution of **1** (1 mM, 200 μL or 400 μL) in chloroform was placed in a 30-mL vial. After the solution was air-dried at ambient temperature under reduced pressure for several hours, 2-propanol or ethanol (8 mL) was added. The mixture was then heated at 50 °C for 2 h and aged at 25 °C overnight. The supernatant in the vial became transparent yellowish brown and was used in the following measurements. Transparent dispersions of **2**, **3**, and **4** were obtained by similar procedures.

Determination of Fullerene-Lipid Concentration in Alcoholic Dispersions

A typical procedure is as follows. Alcoholic dispersions of **2**, **3**, or **4** (each 2 mL) were evaporated, and the residue was dissolved in chloroform (3 mL). We estimated the concentrations of lipids **2**–**4** by employing their molar extinction coefficients at 323 nm in chloroform. UV/Vis spectra were recorded on a Hitachi U-3000 spectrophotometer.

Electron and Atomic Force Microscopic Studies

The alcoholic dispersion (10 μL) was placed by dropper on a carbon-coated copper grid (Ouken Shoji, 200 A mesh), followed by poststaining with uranyl acetate (1 wt% aqueous solution) for TEM (JEOL JEM100S, accelerating voltage = 100 kV). For SEM, (Hitachi S-2250N, accelerating voltage = 20 kV), a mica substrate was immersed in the dispersions in 2-propanol for a few seconds, followed by air-drying. Gold-vapor deposition was conducted before SEM measurements. AFM images were obtained from a mica substrate dipped into the dispersion of **2** in 2-propanol by using an SPI3800N instrument (Seiko Instruments Inc.) in tapping mode.

Dynamic Light Scattering

DLS measurements of the dispersions were conducted at (25 ± 0.5) °C with an Otsuka Electronics Co. LTD ELS-800 instrument. Vertically polarized light from a He–Ne laser (632.8 nm, 10 mW) was directed into the sample cell, and the scattered light was detected at an angle of 90° to the incident beam.

UV/Vis, FTIR, CD, and Raman Spectral Measurements

UV/Vis spectral measurements of the dispersions and lipid cast films were carried out with a JASCO V-570 spectrophotometer or a Hitachi U-3000 spectrophotometer. FTIR spectra of lipid cast films were recorded on a Nicolet Protégé-460 spectrometer (64 scans accumulated for each spectrum). CD spectra for dispersions were recorded on a JASCO J-720 CD spectropolarimeter. A Ramanscope System 1000 instrument (Renishaw) was used for the Raman spectroscopic measurements of the dispersion of **2** before and after photoirradiation with a high-pressure mercury lamp (Irie Science, SHL-100UVQ-2, 75W, irradiation time = 10 h).

X-ray Diffraction

XRD diagrams of cast films of **1** were measured on a Rigaku RINT-2000 diffractometer at room temperature.

Differential Scanning Calorimetry

DSC measurements of a cast film of **1** were carried out at a heating rate of 2.0 °C min^{-1} on a Shimadzu DSC-60 instrument in air or water (20 μL) and in aqueous TEAC (0.5 M, 20 μL).

Electrochemical Measurements

Electrochemical measurements were carried out on a solution of **1** (0.5 mM) in dichloromethane containing tetrabutylammonium perchlorate (0.1 M) and a cast film of **1** on a BPG electrode in aqueous TEAC (0.5 M). A conventional three-electrode configuration was used in both systems. For the solution of **1**, an Au disk and a Pt plate served as the working and counter electrodes, respectively. Ag wire was also used as a pseudo-reference electrode, and the potential was calibrated with the Fc/Fc^+ redox couple. A typical procedure for the preparation of the cast film modified electrode is as follows. A solution of **1** (1 mM, 20 μl) in chloroform was placed on a BPG electrode, and the modified electrode was left to dry in a vacuum desiccator for a day. It was then annealed in the aqueous electrolyte solution at 50 °C for 30 min. A Pt plate and an SCE (Yanaco) were used as the counter and reference electrodes, respectively. CV, DPV, and OSWV measurements were performed with a BAS-100BW electrochemical analyzer. All measurements were carried out with a temperature-controlled electrochemical cell after degassing by bubbling with nitrogen.

Acknowledgements

This work was supported by the 21st Century COE Program "Molecular Informatics" of the Ministry of Education, Culture, Sports, Science, and Technology (Japan) (for N.N.) and by the Kao Foundation for Arts and Science (for H.M.). We are also grateful to Dr. Jonathan P. Hill (NIMS) for his assistance in preparing this manuscript.

[1] W. E. Billups, M. A. Ciufolini, *Buckminsterfullerenes*, VCH, New York, **1993**.
[2] K. Prassides, *Physics and Chemistry of the Fullerenes*, Kluwer Academic, Dordrecht, **1994**.
[3] H. W. Kroto, *The Fullerenes: New Horizons for the Chemistry, Physics and Astrophysics of Carbon*, Cambridge University Press, Cambridge, **1997**.

[4] A. Hirsch, *Fullerenes and Related Structures*, Springer, Berlin, **1999**.
[5] K. M. Kadish, R. S. Ruoff, *Fullerenes: Chemistry, Physics, and Technology*, Wiley, New York, **2000**.
[6] J.-F. Gallani, D. Felder, M. P. Carreon, J.-F. Eckert, D. Gulillon, Y. Rio, J.-F. Nierengarten, *Polym. Mater. Sci. Eng.* **2001**, *54*, 74–75.
[7] H. Murakami, R. Matsumoto, Y. Okusa, T. Sagara, M. Fujitsuka, O. Ito, N. Nakashima, *J. Mater. Chem.* **2002**, *12*, 2026–2033.
[8] D. M. Guldi, *Pure Appl. Chem.* **2003**, *75*, 1069–1075.
[9] N. Nakashima in *Planar Lipid Bilayers (BLMs) and Their Applications, Vol. 7* (Eds.: H. Tien, A. Ottova-Leitmannova), Elsevier, Amsterdam, **2003**, pp. 789–806.
[10] J.-F. Nierengarten, *New J. Chem.* **2004**, *28*, 1177–1191.
[11] H. Imahori, *Org. Biomol. Chem.* **2004**, *2*, 1425–1433.
[12] N. Nakashima in *Encyclopedia of Nanoscience and Nanotechnology, Vol. 3* (Ed.: H. S. Nalwa), American Scientific Publishers, Stevenson Ranch, **2004**, pp. 545–556.
[13] T. Nakanishi, H. Ohwaki, H. Tanaka, H. Murakami, T. Sagara, N. Nakashima, *J. Phys. Chem. B* **2004**, *108*, 7754–7762.
[14] N. Nakashima, M. Sakai, H. Murakami, T. Sagara, T. Wakahara, T. Akasaka, *J. Phys. Chem. B* **2002**, *106*, 3523–3525.
[15] N. Nakashima, N. W. B. Wahab, M. Mori, H. Murakami, T. Sagara, *Chem. Lett.* **2001**, 748–749.
[16] T. Nakanishi, H. Murakami, T. Sagara, N. Nakashima, *Chem. Lett.* **2000**, 340–341.
[17] N. Nakashima, T. Tokunaga, Y. Nonaka, T. Nakanishi, H. Murakami, T. Sagara, *Angew. Chem.* **1998**, *110*, 2817–2818; *Angew. Chem. Int. Ed.* **1998**, *37*, 2671–2673.
[18] N. Nakashima, Y. Nonaka, T. Nakanishi, T. Sagara, H. Murakami, *J. Phys. Chem. B* **1998**, *102*, 7328–7330.
[19] N. Nakashima, T. Kuriyama, T. Tokunaga, H. Murakami, T. Sagara, *Chem. Lett.* **1998**, 633–634.
[20] N. Nakashima, T. Ishii, M. Shirakusa, T. Nakanishi, H. Murakami, T. Sagara, *Chem. Eur. J.* **2001**, *7*, 1776–1782.
[21] T. Nakanishi, M. Morita, H. Murakami, T. Sagara, N. Nakashima, *Chem. Eur. J.* **2002**, *8*, 1641–1648.
[22] T. Nakanishi, H. Murakami, T. Sagara, N. Nakashima, *J. Phys. Chem. B* **1999**, *103*, 304–308.
[23] T. Nakanishi, H. Murakami, N. Nakashima, *Chem. Lett.* **1998**, 1219–1220.
[24] H. Murakami, Y. Watanabe, N. Nakashima, *J. Am. Chem. Soc.* **1996**, *118*, 4484–4485.
[25] D. M. Guldi, F. Zerbetto, V. Georgakilas, M. Prato, *Acc. Chem. Res.* **2005**, *38*, 38–43.
[26] H. Okumura, N. Ide, M. Minida, K. Komatsu, T. Fukuda, *Macromolecules* **1998**, *31*, 1859–1865.
[27] X. Wang, S. H. Goh, Z. H. Lu, S. Y. Lee, C. Wu, *Macromolecules* **1999**, *32*, 2786–2788.
[28] H. Onodera, A. Masuhara, M. Fujitsuka, O. Ito, *Chem. Lett.* **2000**, *2000*, 426–427.
[29] P. Zhou, G.-Q. Chen, H. Hong, F.-S. Du, Z.-C. Li, F. M. Li, *Macromolecules* **2000**, *33*, 1948–1954.
[30] T. Song, S. Dai, K. C. Tam, S. Y. Lee, S. H. Goh, *Polymer* **2003**, *44*, 2529–2536.
[31] T. Song, S. Dai, K. C. Tam, S. Y. Lee, S. H. Goh, *Langmuir* **2003**, *19*, 4798–4803.
[32] S. Dai, P. Pavi, C. H. Tan, K. C. Tam, *Langmuir* **2004**, *20*, 8569–8575.
[33] C. H. Tan, P. Ravi, S. Dai, K. C. Tam, L. H. Gan, *Langmuir* **2004**, *20*, 9882–9884.
[34] M. Sawamura, N. Nagahama, M. Toganoh, U. E. Hackler, H. Isobe, E. Nakamura, S.-Q. Zhou, B. Chu, *Chem. Lett.* **2000**, 1098–1099.
[35] S. Zhou, C. Burger, B. Chu, M. Sawamura, N. Nagahama, M. Toganoh, U. E. Hackler, H. Isobe, E. Nakamura, *Science* **2001**, *291*, 1944–1947.
[36] C. Burger, J. Hao, Q. Ying, H. Isobe, M. Sawamura, E. Nakamura, B. Chu, *J. Colloid Interface Sci.* **2004**, *275*, 632–641.
[37] A. M. Cassell, C. Lee Asplund, J. M. Tour, *Angew. Chem.* **1999**, *111*, 2565–2568; *Angew. Chem. Int. Ed.* **1999**, *38*, 2403–2405.
[38] M. Brettreich, S. Burghardt, C. Böttcher, T. Bayerl, S. Bayerl, A. Hirsh, *Angew. Chem.* **2000**, *112*, 1915–1918; *Angew. Chem. Int. Ed.* **2000**, *39*, 1845–1848.
[39] J. Hao, H. Li, W. Liu, A. Hirsh, *Chem. Commun.* **2004**, 602–603.
[40] M. Sano, K. Oishi, T. Ishi-i, S. Shinkai, *Langmuir* **2000**, *16*, 3773–3776.
[41] V. Georgakilas, F. Pellarini, M. Prato, D. M. Guldi, M. Melle-Franco, F. Zerbetto, *Proc. Natl. Acad. Sci. USA* **2002**, *99*, 5075–5080.
[42] G. Angelini, P. D. Maria, A. Fontana, M. Pierini, M. Maggini, F. Gasparrini, G. Zappia, *Langmuir* **2001**, *17*, 6404–6407.
[43] Z. Shi, J. Jin, Z. Guo, S. Wang, L. Jiang, D. Zhu, *New J. Chem.* **2001**, *25*, 670–672.
[44] H. N. Ghosh, A. V. Sapre, J. P. Mittal, *J. Phys. Chem.* **1996**, *100*, 9439–9443.
[45] R. G. Alargova, S. Degushi, K. Tsujii, *J. Am. Chem. Soc.* **2001**, *123*, 10460–10467.
[46] S. Nath, H. Pal, A. V. Sapre, *Chem. Phys. Lett.* **2003**, *369*, 394–401.
[47] G. Wang, E. Hao, L. Jiao, L. Yan, *Chin. Sci. Bull.* **2003**, *48*, 1938–1942.
[48] S. Shankara Gayathri, A. K. Agarwal, K. A. Suresh, A. Patnaik, *Langmuir* **2005**, *21*, 12139–12145.
[49] T. Nakanishi, W. Schmitt, T. Michinobu, D. G. Kurth, K. Ariga, *Chem. Commun.* **2005**, 5982–5984.
[50] M. Matsumoto, H. Tachibana, R. Azumi, M. Tanaka, T. Nakamura, G. Yunome, M. Abe, S. Tamago, E. Nakamura, *Langmuir* **1995**, *11*, 660–665.
[51] S. Leach, M. Vervloet, A. Després, E. Brèheret, J. P. Hare, T. John Dennis, H. W. Kroto, R. Taylor, D. R. M. Walton, *Chem. Phys.* **1992**, *160*, 451–466.
[52] K. M. Creegan, W. K. Robbins, J. M. Miller, R. D. Sherwood, P. J. Tindall, D. M. Cox, *J. Am. Chem. Soc.* **1992**, *114*, 1103–1105.
[53] L. Isaacs, A. Wehrsig, F. Diederich, *Helv. Chim. Acta* **1993**, *76*, 1231–1250.
[54] A. B. Smith, R. M. Stongin, L. Brard, G. T. Furst, W. J. Romanow, *J. Am. Chem. Soc.* **1993**, *115*, 5829–5830.
[55] M. R. Banks, J. I. G. Cadogan, I. Gosney, P. K. G. Hodgson, P. R. R. Langridge-Smith, P. R. R. Millar, A. T. Taylor, *J. Chem. Soc. Chem. Commun.* **1995**, 885–886.
[56] S. Degushi, R. G. Alargova, K. Tsujii, *Langmuir* **2001**, *17*, 6013–6017.
[57] N. Nakashima, S. Asakuma, T. Kunitake, *J. Am. Chem. Soc.* **1985**, *107*, 509–510.
[58] T. Kunitake, N. Kimizuka, N. Higashi, N. Nakashima, *J. Am. Chem. Soc.* **1984**, *106*, 1978–1983.
[59] A. M. Rao, P. Zhou, K.-A. Wang, G. T. Hager, J. M. Holden, Y. Wang, W.-T. Lee, X.-X. Bi, P. C. Eklund, D. S. Cornett, M. A. Duncan, I. J. Amster, *Science* **1993**, *259*, 955–957.
[60] G. Chambers, H. J. Byrne, *Chem. Phys. Lett.* **1999**, *302*, 307–311.
[61] G. Chambers, K. Henderson, A. B. Dalton, B. McCarthy, H. J. Byrne, *Synth. Met.* **2001**, *121*, 1111–1112.
[62] D. Chapman, *Biomembrane and Functions*, Verlag Chemie, Weinheim, **1984**.
[63] N. Nakashima, N. Yamada, T. Kunitake, J. Umemura, T. Takenaka, *J. Phys. Chem.* **1986**, *90*, 3374–3377.
[64] N. Nakashima, Y. Narikiyo, *Chem. Lett.* **1995**, 653–654.

Received: July 21, 2006
Published online: October 31, 2006

